Lab on a Chip

RSC Publishing

PAPER

Nanobiotechnology advanced antifouling surfaces for the continuous electrochemical monitoring of glucose in whole blood using a lab-on-a-chip†

Cite this: *Lab Chip*, 2013, **13**, 1780

Maria M. Picher,‡[a] Seta Küpcü,[b] Chun-Jen Huang,§[a] Jakub Dostalek,[a] Dietmar Pum,[b] Uwe B. Sleytr[b] and Peter Ertl*[a]

In the current work we have developed a lab-on-a-chip containing embedded amperometric sensors in four microreactors that can be addressed individually and that are coated with crystalline surface protein monolayers to provide a continuous, stable, reliable and accurate detection of blood glucose. It is envisioned that the microfluidic device will be used in a feedback loop mechanism to assess natural variations in blood glucose levels during hemodialysis to allow the individual adjustment of glucose. Reliable and accurate detection of blood glucose is accomplished by simultaneously performing (a) blood glucose measurements, (b) autocalibration routines, (c) mediator-interferences detection, and (d) background subtractions. The electrochemical detection of blood glucose variations in the absence of electrode fouling events is performed by integrating crystalline surface layer proteins (S-layer) that function as an efficient antifouling coating, a highly-oriented immobilization matrix for biomolecules and an effective molecular sieve with pore sizes of 4 to 5 nm. We demonstrate that the S-layer protein SbpA (from *Lysinibacillus sphaericus* CCM 2177) readily forms monomolecular lattice structures at the various microchip surfaces (*e.g.* glass, PDMS, platinum and gold) within 60 min, eliminating unspecific adsorption events in the presence of human serum albumin, human plasma and freshly-drawn blood samples. The highly isoporous SbpA-coating allows undisturbed diffusion of the mediator between the electrode surface, thus enabling bioelectrochemical measurements of glucose concentrations between 500 μM to 50 mM (calibration slope $\delta I/\delta c$ of 8.7 nA mM^{-1}). Final proof-of-concept implementing the four microfluidic microreactor design is demonstrated using freshly drawn blood. Accurate and drift-free assessment of blood glucose concentrations (6. 4 mM) is accomplished over 130 min at 37 °C using immobilized enzyme glucose oxidase by calculating the difference between autocalibration (10 mM glc) and background measurements. The novel combination of biologically-derived nanostructured surfaces with microchip technology constitutes a powerful new tool for multiplexed analysis of complex samples.

Received 27th August 2012,
Accepted 18th February 2013

DOI: 10.1039/c3lc41308j

www.rsc.org/loc

Introduction

The aim of extracorporeal blood therapy is to remove toxic substances from circulation during acute renal failure, sepsis or multiple organ system dysfunctions. To date, extracorporeal blood purification is predominantly used in the replacement of kidney function by hemodialysis and in the support of liver function using adsorptive techniques. However, in the process of dialysis, concentrations of ions such as calcium, potassium, urea and other substances are cleared, including a variety of small molecules such as vitamins and glucose. The removal of glucose from the patient's blood further stresses the body, causing extreme discomfort to the dialysis patient.[1] To counteract the loss of blood sugar, a predefined amount of glucose (1 g L^{-1}) is added to the dialysate during the 2 to 4 h extracorporeal blood purification treatment to prevent energy loss and hyper- or hypoglycemic symptoms. Although the addition of a fixed glucose concentration to the dialysate lessens patient suffering, it does not account for individual variations in blood glucose levels that can range between 0.8 g L^{-1} to 1.8 g L^{-1} within 4 h.[2] The proper adjustment of glucose according to individual patient needs throughout the dialysis process is thus very desirable. The implementation of a feedback loop that continuously assesses blood glucose concentration prior to and after blood purification for the

[a]*AIT Austrian Institute of Technology GmbH, Muthgasse 11/2, 1220 Vienna, Austria. E-mail: peter.ertl@ait.ac.at; Fax: +43 (0) 50550 4450*
[b]*University of Agricultural Resources and Life Sciences, Vienna, Department of Nanobiotechnology (DNBT), Muthgasse 11, 1190 Austria*

† Electronic supplementary information (ESI) available. See DOI: 10.1039/c3lc41308j

‡ Current address: InnerEarLab, Department of Otolaryngology, University of Goettingen, Germany.
§ Current address: Graduate Institute of Biomedical Engineering, National Central University, Jhongli 320, Taiwan.

automated regulation of glucose addition would significantly improve hemodialysis treatment.

Although the benefits of online analysis are evident, advancements in extracorporeal blood glucose monitoring are hindered by the unavailability of low-cost, reliable and drift-free sensors. In this context, portable microdevices, such as lab-on-a-chip (LOC), are well suited for integration into dialysis systems because measurements do not have to be conducted by a skilled operator. Furthermore, LOC systems are capable of rapid and sensitive analysis, and feature improved cost-performance over conventional instrumentation due to parallelization and because less reagents are required.[3–5] The many advantages of LOC technology have made it popular in the past decade and it is applied in immunoassays, detection of toxins in blood, particle sorting and cell analysis. LOC devices are also used for protein synthesis, on-chip PCR, multi-enzymatic assays to detect alcohol levels, as well as lactate[6] and glucose concentrations based on optical[7–11] and electroanalytical techniques.[12–16] Additionally, a large number of LOC devices capable of determining glucose concentrations in whole blood,[16–18] serum, plasma and urine samples[18,19] have been developed using a variety of enzyme immobilization techniques. [20–22]

The integration of electroanalytical techniques, such as amperometric detectors, into microfluidic biochips demonstrate increased spatial and temporal resolution, chemical identification of the substance being detected, low detection limits as well as high sensitivity.[23] We have recently reported the application of amperometric detectors in microfluidic devices to detect biofilm respiration rates based on redox-mediated electrochemical measurements; a principle that has also been used for glucose detection.[24–27] However, the accurate detection of glucose in whole blood samples using amperometric sensors has been hindered by calibration errors, sensor drifts and lag time. While sensor drifts and lag time are common to most biosensors, calibration errors tend to occur when using amperometric sensors because not all of the generated current is specific to glucose. The presence of electroactive components in blood, such as vitamin C *etc.*, creates the need for continuous background measurements and frequent sensor calibrations. Furthermore, long-term monitoring of blood glucose levels is limited by rapid electrode fouling events that occur in protein-rich samples (*e.g.* 70 mg mL^{-1} plasma proteins).[13,28]

To overcome the existing bioanalytical challenges associated with blood glucose monitoring we have developed a lab-on-a-chip that could be employed in a feedback loop mechanism during extracorporeal blood purification. The chip simultaneously performs (a) amperometric blood glucose measurements, (b) autocalibration routines, (c) mediator-interference detection, and (d) background subtractions. All four operating steps are necessary to ensure the continuous, reliable and accurate detection of blood glucose, which relies on enzymatic-based bioelectrochemistry. The key feature of our novel concept is the integration of a uniform bioactive surface layer that is capable of preventing blood coagulation along ''foreign'' LOC surfaces such as glass, PDMS and metal electrodes. In the current work we investigate the crystalline S-layer proteins SbsB and SbpA as bioactive surface components for our microanalytical device because they are compatible with electroanalytical measurement techniques.[29,30] S-layer proteins represent the outermost cell wall component of bacteria and archaea and they perform a variety of important functions, such as acting as precise molecular sieves, providing resistance to heat by increasing membrane stability as well as regulating cell-surface interactions.[31] S-layer lattices are formed by self-assembly and represent a supramolecular cell envelope structure that features pores identical in size and morphology in the 2 to 8 nm range.[32–37] The repetitive feature of the S-layer lattice structure aligns functional groups and pore areas in well-defined positions and orientations at any surface. This means that highly repetitive functional groups are available for binding the monolayers of bioactive molecules such as enzymes, antibodies and immunogens for application in bioanalytical devices, immunoassays, affinity microparticles and affinity membranes.[38–43] Additionally, the intrinsic antifouling characteristics of S-layers have been successfully demonstrated in combination with ultrafiltration membranes (SUMs) where the S-layer protein isolated from *Lysinibacillus sphaericus* CCM 2177 was employed as a molecular sieve exhibiting a cut-off of approx. 30 000 to 40 000 or 4 to 5 nm.[44–48]

The combination of S-layer technology with microfluidics containing embedded amperometric microsensors advances extracorporeal blood glucose monitoring by providing accurate information on blood glucose levels. The nanobiotechnology advanced bioactive microchip surface acts as (1) an efficient immobilization matrix for glucose oxidase (GOx), (2) a uniform antifouling coating to prevent blood from clogging in the microchannels, and (3) a molecular sieve that allows for rapid electron transfer between the electrode surface and the soluble redox-mediator ferricyanide. Since the LOC system allows the prolonged monitoring of glucose during extracorporeal blood purification, the antifouling properties of the S-layer proteins SbpA and SbsB are evaluated against the standard antifouling surfaces, including bovine serum albumin (BSA) and polyethylene glycol (PEG). In this study, chronoamperometric glucose measurements are conducted using protein coated band electrodes, where the 4–5 nm pores of the S-layer lattice structure enable rapid electron transfer between the platinum electrode and GOx, which is covalently attached to the S-layer, using the soluble redox mediator ferricyanide. Additionally, the microfluidic layout consists of two inlets and one outlet that are separated by a microreactor, which is designed for the passive mixing of the redox-mediator solution and blood sample.

Experimental section

Lab-on-a-chip design and fabrication

The entire lab-on-a-chip system (see suppl. information, Fig. 1†) consisted of a microfluidic biochip located in an

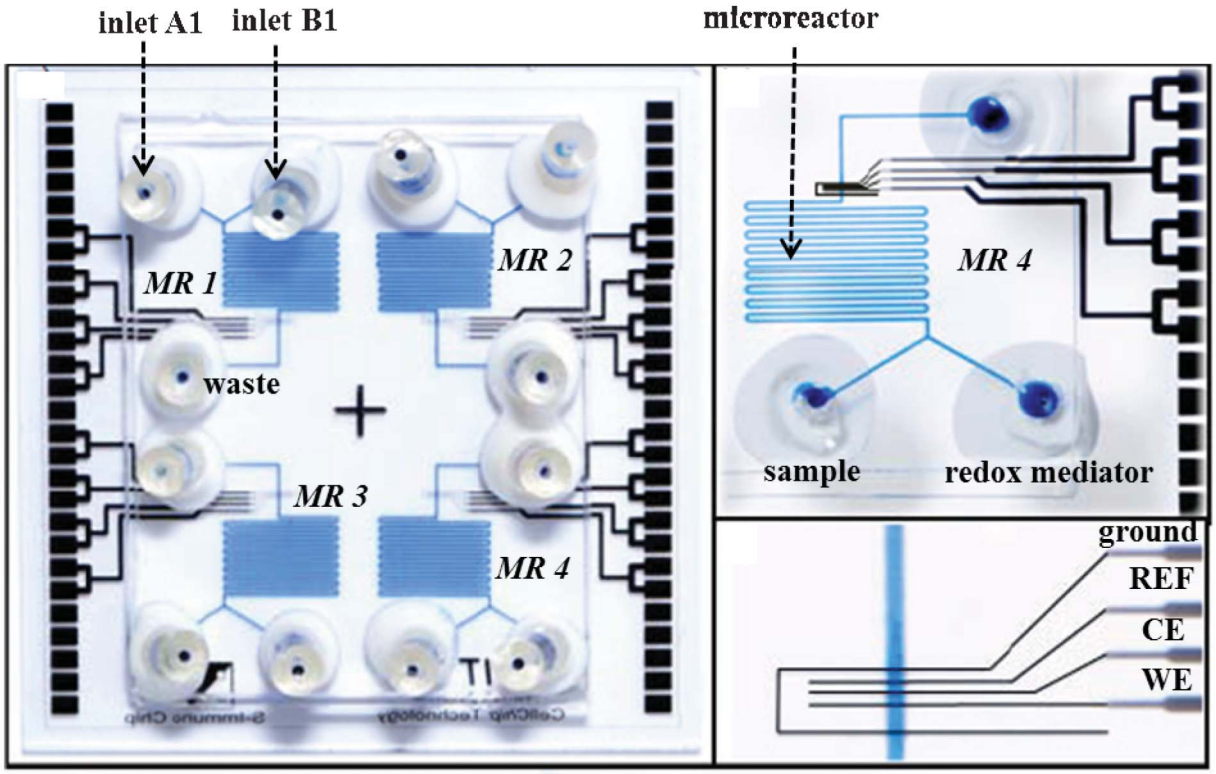

Fig. 1 Images of microfluidic biochip including inlets, wastes, reaction chambers as well as amperometric microsensors located in the end of each microreactor implemented for prolonged blood analysis (MR1), automated background subtraction (MR2), autocalibration (MR3) and drift correction (MR4). Insets show images of 84 mm long microreactor (MR4) separated by two inlets and one waste/outlet as well as electrochemical set up located at the end of each microreactor.

aluminum fixture connected *via* tubing to external valves, injection ports and a syringe pump (KDS 250, KdScientific, USA). The microfluidic biochip was fixed using spring loaded connectors integrated within two printed circuit boards providing shielded connection to the potentiostat (VMP3, Bio-Logic, France). The microfluidic biochip shown in Fig. 1 consisted of a 30 × 30 mm^2 quartz glass substrate (Borofloat®) containing the amperometric sensors and a 15 × 25 mm^2 soft polymer polydimethylsiloxane-based microfluidic (PDMS-Sylgard 184, Dow Corning, Germany). The microfluidic channel layout comprised four individual addressable microreactors of 84 mm length, 30 μm height and 100 μm width. Electrodes, leads and contact pads were fabricated by sputtering a 10 nm titanium seed layer followed by the deposition of a 200 nm platinum layer onto the pre-patterned substrates. The electroanalytical configuration of each microreactor consisted of three band electrodes surrounded by a ground in order to eliminate electrode cross-talk between the four amperometric sensors. Each electrode had a length of 100 μm and 20 μm width. Microfluidic master molds were fabricated by photolithography using the epoxy resin SU8-2050 (height of 30 μm) patterned onto a silicon wafer. Microfluidic channels were formed by pouring a mixture (10 : 1) of PDMS silicone elastomer base and curing agent over the epoxy master molds while polymerization was allowed to take place over a period of 4 h at 70 °C following a 10 min degassing step in a vacuum chamber. The soft polymer fluidic was removed from the master and cut to the appropriate size followed by extensive cleaning using isopropanol and DI water. The pre-cut PDMS microfluidic was aligned under a microscope and put in contact with the bottom substrate immediately after oxygen plasma treatment (Diener Electronics) (30 s at 40 W). A curing time of 24 h at 50 °C was implemented to allow complete cross-linking between the activated PDMS and glass surfaces. Finally a predrilled glass slide was layered on top of the PDMS to mount the self-made injection ports (PEEK tubing 1/32″ and Tygon tube 1/16″, Upchurch Scientific, USA) onto the microfluidic biochip using an epoxy adhesive (35 °C for at least 10 min).

Microchannel surface modification procedures

The S-layer protein SbpA was isolated from cell wall fragments of *Lysinibacillus sphaericus* CCM 2177 as previously described.[49] For recrystallization 2 mg protein lyophilisate were dissolved in 3 mL of 5 M guanidin-hydrochlorid (Gerbu, Germany) in 50 mM TRIS-HCl buffer at pH 7.2 and dialysed against DI water (Millipore, Austria) for 1 h at 4 °C. After dialysis the protein solution was centrifuged for 15 min at 4 °C and the protein concentration was measured using a NanoDrop spectrophotometer (Thermo, Austria) at 280 nm. The S-layer protein stock solution (1 mg mL^{-1} in DI water) was diluted 1 : 10 using a 0.5 mM TRIS buffer containing 10 mM $CaCl_2$ at pH 9; recrystallization was allowed to take place on glass, platinum or PDMS microchip surfaces in the presence of

continuous 0.6 mm s^{-1} fluid flow over a period of 4–12 h at room temperature. Once recrystallization of the S-layer was completed, the microfluidic channels were rinsed with DI water at a flow rate of 0.1 mm s^{-1} for at least 1 h to remove residual S-layer proteins. In case of increased fluid shear stress conditions (*e.g.* flow rates above 2 mm s^{-1}), the recrystallized S-layer was further stabilized by inter- and intramolecular covalently linking protein subunits using the cross-linkers like glutardialdehyde (GA), bis(sulfosuccinimidyl) suberate (BS^3) and dimethyl pimelimidate (DMP). S-layer stabilization using GA was performed by incubating 0.5% GA in 0.1 M PBS for 30 min and Schiff bases were reduced by using 10 mM sodium borohydride ($NaBH_4$) in a 10 mM NaOH solution for 50 min. The BS^3 cross-linking procedure began with a 30 min incubation period for S-layer proteins with 1.7 mM BS^3 in 20 mM PBS and followed by a 15 min washing step using a 1M TRIS buffer (pH 7.5) to quench unreacted BS^3. DMP cross-linking was performed using a HEPES buffer (pH 8) containing 10 mM DMP followed by a 60 min incubation period. Stabilization of the S-layer protein crystal was accomplished by cross-linking available amino groups. The remaining free carboxyl groups were activated using 10 mM 1-ethyl-3-(3-dimethylaminopropyl)carbodiimide hydrochloride (EDC) in DI water at pH 4.75 for 1 h, rinsed with cold DI water and subsequently incubated with the 400 μg mL^{-1} GOx solution for 12 h. Following the immobilization of GOx onto the S-layer protein, the functionalized surface was rinsed with cold PBS for approx. 2 h.

S-layer characterization using SPR

The antifouling properties of surfaces modified with SbpA and SbsB S-layer proteins, as well as by PEG and BSA in the presence of the HSA, human plasma and whole human blood were evaluated using surface plasmon resonance spectroscopy (SPR). While the surface protein SbsB originates from *Bacillus stearothermophilus* PV72/p2 and forms oblique lattice structures, SbpA originates from *Lysinibacillus sphaericus* CCM 2177 (*syn*. *Lysinibacillus sphaericus* CCM 2120) and forms square lattices following surface crystallization. The in-house built SPR system is described in detail elsewhere (see suppl. information, Fig. 4†).[50] In brief, a 50 nm gold coated glass sensor chip was optically matched on top of a prism and the flow chamber (10 μL volume, 1 cm length and 100 μm depth) was pressed against the gold surface to form a tight seal. The microfluidic sensor chip and prism coupler were mounted on a rotational stage (2-circle 414, Huber AG, Germany) to adjust the angle of incidence of the laser beam, while the intensity of the reflected laser beam was measured using a photodiode connected to a lock-in amplifier (Model 5210, Princeton Applied Research, USA). Following recrystallization of the SbpA protein at the gold surface, the flow chamber was rinsed using the above described protocol. For SbsB protein recrystallization on the gold surface a protein solution of 100 μg mL^{-1} in Hank's Balanced Salt Solution (HBSS; PAA, Austria) pH 7.2 was used. After a 12 h recrystallization period, the gold surface was rinsed with DI water. The amount of non-specifically adsorbed molecules was quantified in terms of surface mass density (ng mm^{-2}) in the presence of 30 mg ml^{-1} HSA in 0.5 mM TRIS buffer (pH 7.5), human plasma and whole human blood for a period of 1 h at 200 μL min^{-1} flow rate. Results of the study were compared with standard antifouling surfaces including PEG and BSA surfaces. PEG surfaces were made using gold coated glass slides that were incubated with a thiol-PEG solution (1 mM PEG in ethanol) for 24 h to form a self-assembled monolayer (SAM) and then extensively rinsed with ethanol and dried using inert argon. PEG-covered biochips were stored in an argon filled glass box and sealed with parafilm. For BSA covered gold surfaces, 30 mg mL^{-1} BSA in PBS was allowed to adsorb onto the gold-covered glass slides for a period of 1 h prior to use.

Microfluidic electrochemical measurements using microelectrodes

Unless otherwise stated, oxidation currents of the redox indicator couple ferro/ferricyanide (60 mM) at the S-layer coated platinum or gold band electrodes were monitored with an adjusted flow velocity of 1.7 mm s^{-1} using chronoamperometry by setting the working electrode (WE) at +0.45 V *versus* the internal reference (REF) and counter electrodes (CE). Both electrode materials (Pt and Au) showed comparable FCN oxidation currents at +0.45 V using the current electrode configuration. The resulting oxidation currents are an indication of glucose concentration.

A written consent form was obtained from the human subject that provided the blood samples for this study. All experiments involving whole blood analysis were performed in compliance with the relevant laws and institutional guidelines of the AIT Austrian Institute of Technology, GmbH.

Results and discussion

Surface protein (S-layer) coating analysis

The purpose of the developed microfluidic platform is the long-term, continuous and interference-free monitoring of blood glucose concentrations using enzyme-based bioelectrochemistry. A prerequisite to conducting electrochemical measurements of whole blood in microfluidic devices is the integration of a uniform antifouling coating to prevent unwanted interactions (*e.g.* biofouling) at the various microchip surfaces. Although a variety of different antifouling strategies for microfluidic devices have been proposed in recent years, technological limitations have hindered their broader application.[51–54] For instance, the combination of antifouling layers with microfluidic technologies containing embedded electroanalytical microsensors requires the complete (*e.g.* pin-hole free) modification of different microchip surfaces such as glass (bottom substrate), metals (electrodes) and polymers (microfluidics) while simultaneously recording electrochemical signals of the fully covered electrode surface. In this case only the S-layer technology is capable of forming a well-defined protein monolayer that features precise pores and allows for sufficient electron-transfer to take place between the soluble redox-mediator and the working electrode.

In this study the S-layer proteins SbsB and SbpA were employed as novel antifouling layers to cover the microfluidic channel network consisting of glass (bottom) and PDMS (walls

and top) as well as the metal electrodes. The S-layer protein layer was characterized using atomic force microscopy (AFM), cyclic voltammetry (CV), fluorescent imaging and surface plasmon resonance spectroscopy (SPR). AFM images taken after recrystallization confirmed the formation of a well-defined protein monolayer that features a lattice structure on glass, platinum or gold and PDMS surfaces (see suppl. information, Fig. 2 and 3a†). Next, the ability to conduct electrochemical measurements in the presence of S-layer coated working electrodes was investigated using commercially available disk-electrodes (1 mm dia.) and electrochemical set-up (BAS). Results of this study demonstrated that the large number of well-defined pores of the S-layer coating allow for efficient FCN diffusion to the electrode surface (see suppl. information, Fig. 3b†). To further confirm S-layer formation within the microchannels, fluorescence imaging was used to assess the protein SbpA coating by means of immunolabelling using the anti SbpA_IgG and anti IgG_TRITC affinity complex. Obtained fluorescence images (see suppl. information, Fig. 4c†) of the microfluidic channel network taken at increasing focal points indicated the formation of recrystallized S-layers along the glass bottom, PDMS side and top walls. Additional surface plasmon resonance spectroscopy (SPR) measurements were conducted to characterize S-layer adsorption processes and their stability under constant flow conditions. Results shown in Fig. 2 (see also suppl. information, Fig. 4†) demonstrate the formation of protein monolayers of approx. 9 nm (SbpA) and 4 nm (SbsB) in thickness [55,56] within 60 min under flow conditions.[66,67]

Furthermore, the protein monolayers remained stable over a period of 400 min following exposure to human plasma, whole blood and 60 mg mL^{-1} HSA. In a subsequent comparative analysis, those three electrode fouling solutions were tested against six modified gold surfaces carrying native or stabilized (*e.g.* GA, BS^3 and DMP cross-linker) SbpA and SbsB S-layers, as well as thiol-PEG and BSA antifouling layers. Antifouling characteristics are listed in Table 1 where obtained surface mass density of adsorbed molecules (ng mm^{-2}) after 90 min incubation with human plasma, 30 mg mL^{-1} HSA and whole blood samples were calculated from SPR data. SPR results show that S-layer SbpA exhibits superior antifouling properties over PEG, BSA and SbsB modified gold surfaces. Although it is not entirely clear which specific SbpA property (*e.g.* surface charge, pore size or composition) is responsible for the 90% decrease in surface adsorption (0.46 ng mm^{-2}) compared with bare gold surfaces (4.44 ng mm^{-2}) using whole blood, it is known that SbpA acts as an efficient diffusion barrier for molecules larger than 4 nm.[44]

Although we successfully demonstrated that the redoxactive compound FCN is capable of freely crossing the SbpA diffusion barrier, a variety of electron transfer mediators were tested to find the most suitable enzyme-mediator couple. Ideal redox mediators are normally small soluble molecules capable of accessing the active site of the respective redox-enzyme and that can undergo fast reversible oxidation and reduction reactions at the electrode surface. Another important characteristic of redox mediators is long-term enzyme stability in the presence of mediator excess (up to 100 fold). To test GOx stability, a series of experiments were initially performed using

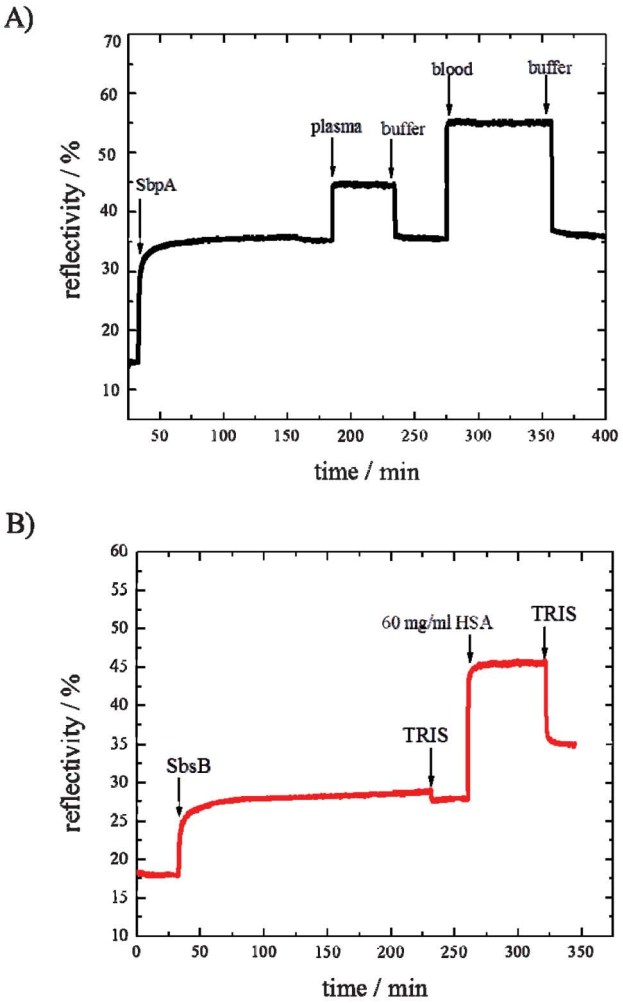

Fig. 2 (A) S-layer formation dynamics and antifouling properties of crystalline SbpA in the presence of human plasma and whole blood. (B) S-layer formation dynamics and antifouling properties of crystalline SbsB coating in the presence of 60 mg mL^{-1} HSA.

the redox mediators hydroquinone, ferricyanide, 8-hydroxyquinoline, anthraquinone and menadione. Results employing a commercial electrochemical set-up are listed in suppl. information Table 1, ESI†, which show highest remaining GOx activity at 96% after 24 h using 1 mM ferricyanide, while the lowest GOx activity was set at 79% using 1 mM anthraquinone. Additionally, unspecific redox reactions and amperometric background currents of each GOx-mediator couple were measured in the absence of glucose. Similar to GOx activity results, ferricyanide showed the highest signal-to-noise (S/N of 93 : 1 in the presence and absence of glucose) ratio while anthraquinone and hydroquinone exhibited the lowest S/N ratios at 80 : 1 and 2 : 1, respectively. Further analysis of enzyme kinetics in the presence of a fixed 200 mM glucose concentration also showed highest amperometric signals with increasing concentrations of 10–50–100 μg mL^{-1} GOx when using 60 mM FCN (see suppl. information, Table 2†). Consequently, the final enzyme-coupled bioelectrochemistry detection system employed 60 mM FCN to mediate

Table 1 Comparative analysis of various antifouling layers using SPR following 90 min exposure to human plasma, 60 mg mL^{-1} human serum albumin and human blood

Antifouling layer	Human plasma/ng mm^{-2}	Human serum albumin/ng mm^{-2}	Human blood/ng mm^{-2}
Plain Au surface	3.74	n.a.	4.44
SbpA	0.18[a]	0	0.46
SbsB	2.46	1.34	n.a.
SbpA-GA stabilized	0.18[a]	n.a.	n.a.
SbpA-BS^3stabilized	1.02[a]	n.a.	n.a.
SbpA-DMP stabilized	0.75[a]	n.a.	n.a.
PEG	0.76	0.41	n.a.
BSA	1.92	n.a.	n.a.

[a] Triplicate measurements exhibited a RSD of approx. 10%.

the electron transfer between the GOx active site and the electrode surface.

Microreactor testing and optimization of microfluidic electrochemical set up

The electrochemical measurement set-up was optimized using a defined FCN solution in the presence of increasing flow velocities and temperature profiles. Results shown in Fig. 3a and 3b revealed highest oxidation currents at an applied potential of +450 mV, a detection limit (DL) of approx. 100 μM ferrocyanide and linear range (LR) between 500 μM to 50 mM (calibration slope $\delta I/\delta c$ of 8.7 nA mM^{-1}). Additional investigation of temperature and flow-dependent signal changes revealed approx. 1.5 nA $°C^{-1}$ signal change (*e.g.* ΔI +16 nA from room temperature to 37 °C) and a non-linear signal increase of ΔI of 21 nA, 8 nA and 2 nA following flow increases from 1.7 mm s^{-1} to 16.7 mm s^{-1} to 72.4 mm s^{-1} and to 128.0 mm s^{-1} (see suppl. information Fig. 5†). These results further demonstrate the importance of controlling critical measurement parameters, including temperature, flow velocities and applied potentials during continuous extracorporeal blood glucose detection. Another important aspect of performing enzyme catalyzed reactions in microfluidic channels is the optimization of resident time to allow sufficient interaction to occur between the GOx, glucose and redox-mediator mixture. As shown in Fig. 1, four microreactors (V_{total} 250 nL) 84 mm in length and of serpentine shape were implemented to enable the efficient mixing of glucose, GOx and redox-mediator. The calculated fluid velocities inside the microreactors in the presence of 0.35 μL min^{-1} flow rate yielded an average fluid velocity (u_{avg}) of 2000 μm s^{-1} and a maximum fluid velocity (u_{max}) of 3000 μm s^{-1} in the center of the parabolic flow profile (z = 15 μm). Mixing rates within the microreactors were initially calculated based on previously described molecular diffusion coefficients for GOx and ferricyanide of 4.5×10^{-11} m^2 s^{-1} and of 8×10^{-10} m^2 s^{-1}, respectively.[57] Additional CFD simulations showed that the complete mixing of a 100 μg mL^{-1} GOx solution with 60 mM ferricyanide can be achieved within the first 28 mm (or one third of the microchannel) at 2000 μm s^{-1} fluid flow (see suppl. information, Fig. 6). To experimentally evaluate the performance of the serpentine microreactor, on-chip glucose detection was compared with results obtained using a commercially available ''Tee-micromixer'' (Upchurch Scientific, USA). In both cases enzymatic reaction rates are assessed using amperometric microelectrodes following the injection of a GOx (200 μg mL^{-1}) solution through inlet A and a redox-mediator solution (120 mM ferricyanide) containing 20 mM glucose through inlet B. While similar reaction rates were obtained at 1.67 mm s^{-1} flow velocities, a significant decrease in amperometric current signals was observed with fluid rates of 5.7 mm s^{-1} (60%) and 16.7 mm s^{-1} (52%) using the serpentine microreactor (see suppl. information, Table 3, ESI†). These results indicate that the mixing capacities of the microfluidic microreactor for soluble GOx enzymes is strongly dependent on flow rates while the commercial micromixer showed stable oxidization currents of approx. 30 nA up to a fluid rate of 5.7 mm s^{-1}. Final optimization of microfluidic flow conditions involved the repeated injection of 20 mM glucose into a constant stream of enzyme-mediator solution containing 200 μg mL^{-1} GOx and 120 mM FCN, respectively. Fig. 3c shows current-time traces obtained at 1.67 mm s^{-1}, 5.7 mm s^{-1}, 11.3 mm s^{-1} and 16.7 mm s^{-1} fluid flow velocities. Results demonstrate improved enzymatic reaction rates with lower flow rates, exhibiting an approximate 10 fold signal increase (*e.g.* 13 nA to 160 nA) when reducing flow velocity from 16.7 mm s^{-1} to 1.67 mm s^{-1}. The poor reproducibility of the individual peak values was likely caused by pressure differences at the Y-intersection of inlet A and B (see Fig. 1) when switching the syringe pumps.

In a first attempt to demonstrate the feasibility of the long-term amperometric monitoring of glucose using SbpA-coated microreactors, the enzyme-mediator mixture (150 μg mL^{-1} GOx containing 60 mM FCN) was introduced in inlet A while human plasma (courtesy of the AKH) was pumped through inlet B into the microreactor at 1.67 mm s^{-1}. Fig. 4a shows current-time traces obtained from two parallel operated microreactors each containing glucose-spiked (1 mg mL^{-1}) human plasma in the (i) presence and (ii) absence of the GOx-containing mediator solutions (background measurement). Although the observed amperometric signal decrease within the first 80 min in the presence of 5 mM glucose-spiked plasma samples cannot be easily explained, it may be attributed to a loss of enzymatic activity of the freshly prepared enzyme-mediator (GOx-FCN) solution. Additional experiments (data not shown) revealed stable amperometric signals for over 5 h using a soluble GOx-mediator solution following an initial adjustment period of approx. 60 min at room temperature. In a subsequent comparative analysis (see Fig. 4b), amperometric

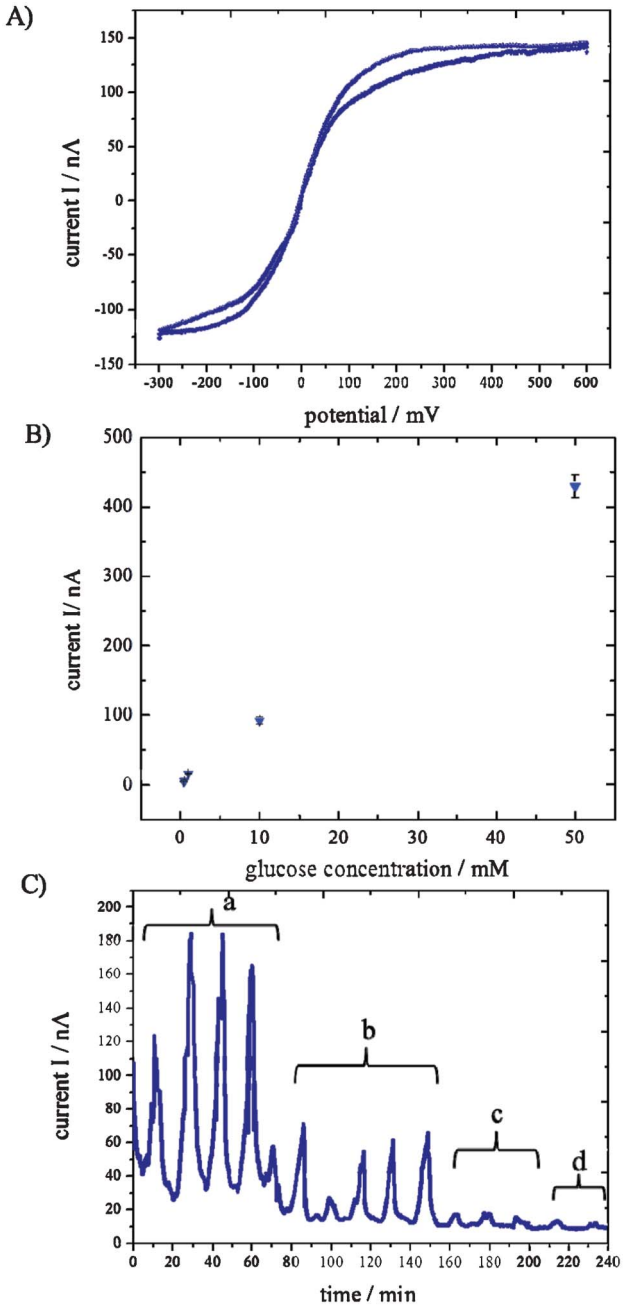

Fig. 3 (A) Cyclic voltammetry (CV) of 60 mM FCN solution using band microelectrodes in the absence of flow. (B) Concentration dependent amperometric currents obtained after triplicate measurements using increasing concentration of glucose in the presence of 60 mM FCN and 150 μg mL^{-1} soluble GOx. (C) Current-time traces (nA) obtained following subsequent injections of 20 mM glucose into a 100 μg mL^{-1} GOx/60 mM FCN solution at (a) 1.7 mm s^{-1}, (b) 5.7 mm s^{-1}, (c) 11.3 mm s^{-1} and (d) 16.7 mm s^{-1} fluid flow velocities.

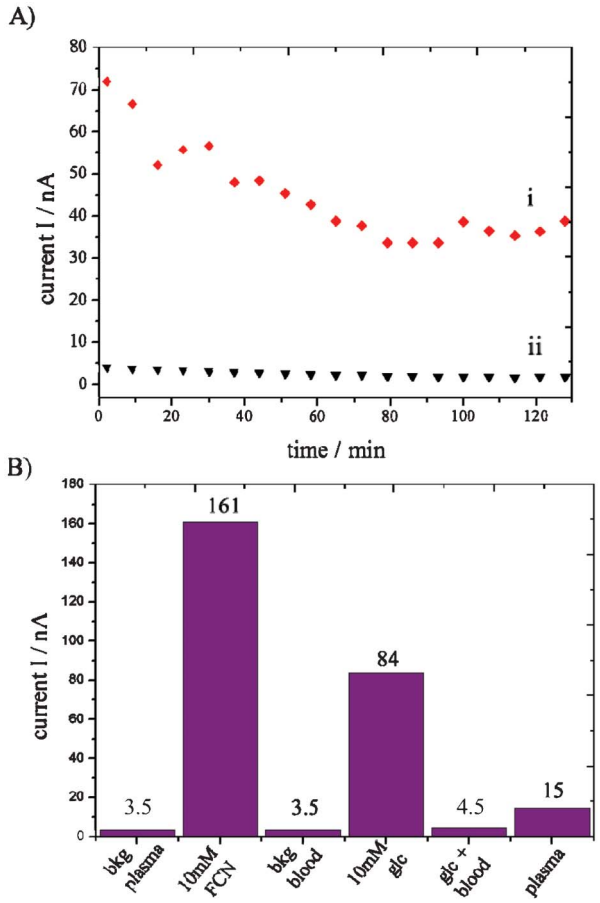

Fig. 4 (A) Current time traces obtained after 120 min from 2 microreactors, each containing glucose-spiked (1 mg mL^{-1}) human plasma (inlet A) in the presence (i) and absence (ii) of the GOx-containing mediator solutions (inlet B). Amperometric signals were sequentially recorded every 5 min following a two minute measurement period and a time delay of 1 min between both microreactors to eliminate possible electrode cross-talk. (B) Amperometry using 3 electrode configuration of buffer containing either10 mM FCN or 5 mM glucose, human plasma and whole blood samples as well as glucose-spiked human plasma and glucose-spiked whole blood human samples.

signals obtained after 120 min continuous flow of plasma and whole blood were evaluated using a commercially available glucose sensor (Accu-Check, Roche). While the calculated glucose concentration of approx. 1.15 mM (14.7 nA) in plasma corresponded well with values obtained using the commercial sensor, a significantly reduced sensor response was found when using freshly drawn blood (3.5 nA or 0.26 mM glc) and 1 mg mL^{-1} glucose-spiked whole blood (4.5 nA or 0.35 mM glc) (see also suppl. information, Fig. 7, ESI†). These results indicate a possible inactivation of the soluble GOx in the presence of whole blood since additional mediator-blood interference studies showed no measurable effects on FCN detection (data not shown).

Immobilized glucose oxidase and blood testing

To minimize the effects of whole blood–enzyme interactions and to improve amperometric signals, the GOx enzyme was covalently linked to the S-layer coated microchannels. The crystallized surface protein SbpA layer was found ideally suited as an immobilization matrix for GOx due to its high number of free carboxyl groups available to attach bioactive molecules using well-known protein conjugation techniques. Four GOx immobilization protocols were investigated and compared

Table 2 Optimization of the GOx immobilization procedure at the SbpA-antifouling layers

	Oxidation currents after 5 min reaction with 60 mM FCN		
Cross-linking reagent	NO glucose	10 mM glucose	ΔI
EDC	3 nA	92 nA	89 nA
BS^3-EDC	3 nA	76 nA	73 nA
DMP-EDC	3 nA	98 nA	95 nA
GA-EDC	15 nA	93 nA	78 nA

using static chronoamperometric measurement conditions. Here, four PDMS wells were placed over the three electrode set-up of the biochip and SbpA was recrystallized and subsequently pre-treated with GA (well 1), BS^3 (well 2) and DMP (well 3), followed by EDC activation and covalent linking of GOx to the SbpA. Additionally, GOx immobilization was carried out using EDC without the pre-treatment procedure intended for S-layer stabilization was investigated in the remaining PDMS well (well 4). Table 2 lists the results for the four immobilization protocols showing amperometric currents obtained after a 5 min reaction time following the addition of 10 mM glucose and 60 mM FCN. Highest signal increases were found after the initial DMP treatment and EDC-coupling of GOx onto the SbpA monolayers. Fig. 5a shows current–time traces of blood glucose measurements using the DMP-EDC-GOx functionalization protocol. While whole blood backgrounds were obtained in the absence of FCN mediator solution (bkg of 2.4 nA), the addition of 10 mM glucose increased amperometric signals to 9.5 nA and subsequent injection of freshly drawn whole human blood samples decreased the current to 6.6 nA corresponding to approx. 4.0 mM blood glucose. Although the resulting amperometric signals are in the low nA range, the obtained differences in current–time traces between blood background, 10 mM glucose solution and freshly drawn blood indicate that it is indeed feasible to monitor physiological blood glucose levels (see Fig. 5b). The final proof-of-concept was performed using freshly drawn human blood. An important feature of the lab-on-a-chip is the integration of four microreactors to simultaneously monitor blood glucose, blood background, pure glucose and FCN, thus allowing for integrated autocalibration and sensor drift corrections. However, prior to conducting whole blood analysis, equivalent mixing performance and sensor to sensor variations were determined for each of the four microreactors. Results shown in Fig. 6a indicate a 5% signal variation after 50 min (85 ± 4 nA) between the four microreactors following the mixing of a 50 mM glucose with a 120 mM FCN solution containing 300 μg mL^{-1} soluble GOx. To conduct whole blood analysis, freshly drawn human blood, glucose, FCN and buffer solutions were connected *via* external tubing and valves to the syringe pump according to the following configuration (see also Fig. 1):

Microreactor 1: *inlet* 1A: blood & *inlet* 1B: 120 mM FCN → blood glucose.

Microreactor 2: *inlet* 2A: blood & *inlet* 2B: buffer → background.

Microreactor 3: *inlet* 3A: 20 mM glc & *inlet* 3B: 120 mM FCN → calibration.

Microreactor 4: *inlet* 4A: buffer & *inlet* 4B: 120 mM FCN → drift correction.

Fig. 6b shows stable current-time traces in the presence of blood (MR1 at 25 nA), buffer (MR2 at 6 nA), FCN (MR4 at 9 nA) and 10 mM glucose (MR3 at 30 nA) solutions measured over a period of 130 min at 37 °C. The amperometric signal differences between blood background, blood sample and glucose calibration puts glucose concentration at an estimated 6.4 mM in the freshly drawn blood sample. These results demonstrate the ability of integrated S-layer coating to act as an efficient antifouling layer, effective immobilization matrix for enzyme coupled bioelectrochemistry and precise molecular

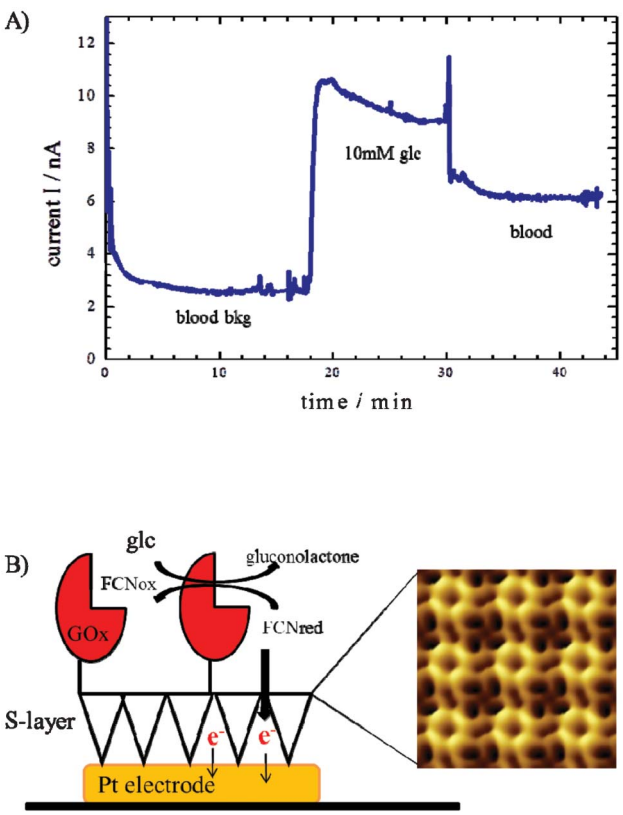

Fig. 5 (A) Amperometric-time traces using S-layer immobilized GOx following the subsequent injections of whole blood in the absence of FCN mediator solution (0 to 18 min), 10 mM glucose (19 to 29 min), and freshly drawn whole human blood samples (30 to 42 min). (B) Schematic drawing of the sensor layout containing S-layer and immobilized GOx-enzyme. Enzyme immobilization is achieved by EDC-coupling of GOx onto the SbpA monolayers following an initial DMP treatment to stabilize the S-layer.

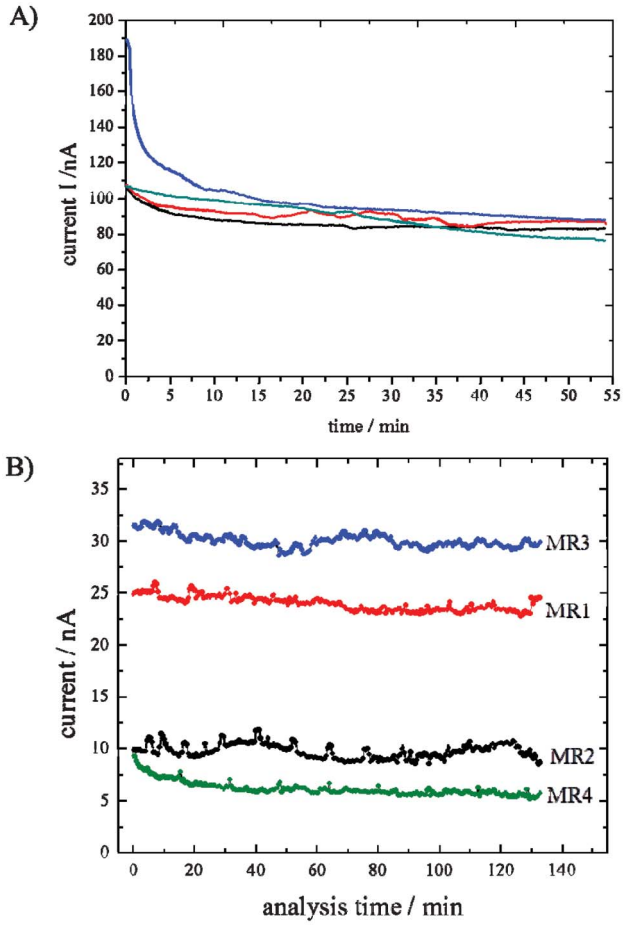

Fig. 6 (A) Current-time traces obtained from SbpA-coated microreactors 1 to 4 following the addition of 50 mM glucose though inlet A and 120 mM FCN solution containing 300 μg mL^{-1} soluble GOx through inlet B. (B) Amperometric current-time traces obtained over a period of 130 min at 37 °C using 4 microreactors containing bioactive (GOx-coupled) antifouling layers of freshly drawn blood (MR1 and MR2), 10 mM glucose for autocalibration (MR3) and 120 mM FCN mediator solution (MR4).

sieve allowing only access of small soluble compounds such as the electroactive FCN to the electrode surface.

Conclusions

We have developed a lab-on-a-chip to detect glucose concentrations in whole human blood to advance existing extracorporeal blood purification methods. It is envisioned that the lab-on-a-chip could be used in a feedback loop to assess the natural variations in blood glucose levels during hemodialysis and thus lessen patient discomfort by allowing the individual adjustment of glucose. The proposed lab-on-a-chip combines nanobiotechnology with microchip technology by using the bacterial cell wall protein SbpA as a uniform surface coating that functions as an efficient antifouling layer and immobilization matrix for enzymes. SbpA protein monolayer stability, surface coverage and improved antifouling properties over conventional antifouling strategies such as PEG and BSA were demonstrated using surface plasmon resonance spectroscopy. Measurements conducted under various flow conditions revealed that the SbpA (from *Lysinibacillus sphaericus* CCM 2177) functions as an efficient antifouling layer for whole blood samples. The observed outstanding antifouling characteristics of SbpA in the presence of high-protein solutions (70 mg mL^{-1} HSA), plasma and whole blood samples is explained by the inherently neutral surface charge of the protein. AFM images and immunofluorescent labeling methods confirmed the ability of SbpA proteins to readily recrystallize onto various microchip surfaces including glass, metals and polymers with sufficient stability. Furthermore, the straightforward recrystallization procedure leading to the formation of homogenous monolayers makes S-layers an ideal surface coating method for microfluidic applications. Another advantage of integrating a SbpA layer into microfluidic channels containing embedded electroanalytical sensors is that it makes the transport of small soluble redox molecules through the large number of pores (4 nm dia.) to the electrode surface possible. Cyclic voltammetry measurements also confirmed the ability of SbpA-coated microelectrodes to measure electrochemical oxidation and reduction reactions in the presence of FCN.

The SbpA-coating was integrated into a four channel configuration, each containing an embedded amperometric microsensor located after each microreactor, to continuously detect glucose concentrations, background contributions, sensor drifts and interferences. While microchip technology allows precise control over microreactor geometry, temperature profiles, and flow velocities for optimized enzyme–glucose–mediator interaction kinetics, the SbpA-coated electrodes provide stable and reproducible amperometric signals over long periods of time. The developed microfluidic device provided stable, reliable and accurate detection of glucose in human plasma, but measurements performed using freshly drawn blood indicated an inactivation of soluble GOx. The GOx enzyme was therefore covalently linked to the SbpA-coated microchannels to improve amperometric signals. A final proof-of-concept showed that continuous whole blood glucose measurements, autocalibration, background subtractions and drift corrections can be simultaneously performed using GOx immobilized SbpA-based antifouling layers. Although the continuous monitoring of blood glucose variations in combination with extracorporeal blood purification was not performed, obtained results demonstrate that it would be possible to integrate the microchip-based feedback loop into a hemodialysis system. The ability to conduct drift-free and reliable electrical measurements using whole human blood samples has the potential to significantly advance blood analysis.

Acknowledgements

The authors would like to thank Prof. Vienken for his valuable input on extracorporeal blood purification and ideas relating to blood glucose monitoring. Financial support received from the Center of Innovation and Technology (ZIT), Vienna, Austria, is greatly acknowledged. Microfabrication was carried

out in the clean rooms of the Center of Micro- and Nanostructures, Vienna University of Technology.

References

1 E. Sobngwi, G. Ashuntantang, E. Ndounia, M. Dehayem, M. Azabji-Kenfack, F. Kaze, E. Balti and J. C. Mbanya, *Diabetes Res. Clin. Pract.*, 2010, **90**(1), 22–25.
2 J. R. Castle and W. K. Ward, *J Diabetes Sci Technol*, 2010, **4**(1), 221–5.
3 G. Birnbaumer, S. Kupcu, C. Jungreuthmayer, L. Richter, K. Vorauer-Uhl, A. Wagner, C. Valenta, U. Sleytr and P. Ertl, *Lab Chip*, 2011, **11**(16), 2753–2762.
4 G. M. Birnbaumer, P. A. Lieberzeit, L. Richter, R. Schirhagl, M. Milnera, F. L. Dickert, A. Bailey and P. Ertl, *Lab Chip*, 2009, **9**(24), 3549–56.
5 C. Rivet, H. Lee, A. Hirsch, S. Hamilton and H. Lu, *Chem. Eng. Sci.*, 2011, **66**(7), 1490–1507.
6 I. Moser, G. Jobst and G. A. Urban, *Biosens. Bioelectron.*, 2002, **17**(4), 297–302.
7 H. Han, Y. Li, H. Yue, Z. Zhou, D. Xiao and M. M. F. Choi, *Clin. Chim. Acta*, 2008, **395**(1–2), 155–158.
8 A. Pasic, H. Koehler, L. Schaupp, T. R. Pieber and I. Klimant, *Anal. Bioanal. Chem.*, 2006, **386**, 1293–1302.
9 Z. Zhou, L. Qiao, P. Zhang, D. Xiao and M. M. F. Choi, *Anal. Bioanal. Chem.*, 2005, **383**, 673–679.
10 M. Pleitez, H. von Lilienfeld-Toal and W. S. Mäntele, *Spectrochim. Acta, Part A*, 2012, **85**(1), 61–65.
11 J. Y. Kim, J. Y. Baek, H. H. Kim, K. A. Lee and S. H. Lee, *Sens. Actuators, A*, 2006, **128**(1), 7–13.
12 R. Kurita, K. Hayashi, X. Fan, K. Yamamoto, T. Kato and O. Niwa, *Sens. Actuators, B*, 2002, **87**(2), 296–303.
13 B. U. Moon, S. Koster, K. J. Wientjes, R. M. Kwapiszewski, A. J. Schoonen, B. H. Westerink and E. Verpoorte, *Anal. Chem.*, 2010, **82**(16), 6756–63.
14 J. Wang, M. P. Chatrathi and B. Tian, *Anal. Chem.*, 2001, **73**(6), 1296–300.
15 S. Böhm, D. Pijanowska, W. Olthuis and P. Bergveld, *Biosens. Bioelectron.*, 2001, **16**(6), 391–397.
16 S. Milardović, I. Kruhak, D. Iveković, V. Rumenjak, M. Tkalčec and B. S. Grabarić, *Anal. Chim. Acta*, 1997, **350**(1–2), 91–96.
17 V. Sanz, S. de Marcos and J. Galbán, *Biosens. Bioelectron.*, 2007, **22**(12), 2876–2883.
18 V. Srinivasan, V. K. Pamula and R. B. Fair, *Lab Chip*, 2004, **4**(4), 310–315.
19 V. Srinivasan, V. K. Pamula and R. B. Fair, *Anal. Chim. Acta*, 2004, **507**(1), 145–150.
20 M. R. Guascito, D. Chirizzi, C. Malitesta, M. Siciliano, T. Siciliano and A. Tepore, *Electrochem. Commun.*, 2012, **22**, 45–48.
21 X. Cao and N. Wang, *Analyst*, 2011, **136**, 4241–4246.
22 J. Wang, W. Bao and L. Zhang, *Anal. Methods*, 2012, **4**, 4009–4013.
23 C. Amatore, N. Da Mota, C. Sella and L. Thouin, *Anal. Chem.*, 2008, **80**(13), 4976–4985.
24 J. Gottschamel, L. Richter, A. Mak, C. Jungreuthmayer, G. Birnbaumer, M. Milnera, H. Bruückl and P. Ertl, *Anal. Chem.*, 2009, **81**(20), 8503–8512.
25 E. H. Yoo and S. Y. Lee, *Sensors*, 2010, **10**(5), 4558–4576.
26 L. Luo, Q. Li, Y. Xu, Y. Ding, X. Wang and D. Deng, *Sens. Actuators, B*, 2010, **145**(1), 293–298.
27 B. Kovatchev, S. Anderson, L. Heinemann and W. Clarke, *Diabetes Care*, 2008, **31**(6), 1160–4.
28 H. Lerner, J. Giner, J. S. Soeldner and C. K. Colton, *J. Electrochem. Soc.*, 1979, **126**(2), 237–242.
29 A. Neubauer, C. Hodl, D. Pum and U. B. Sleytr, *Anal Lett*, 1994, **27**(5), 849–865.
30 A. Neubauer, D. Pum and U. B. Sleytr, *Anal. Lett.*, 1993, **26**(7), 1347–1360.
31 U. B. Sleytr, B. Schuster, E. M. Egelseer, D. Pum, C. M. Horejs, R. Tscheliessnig and N. Ilk, in *Progress in Molecular Biology and Translational Science*, ed. S. Horworka, 2011, vol. 103, pp. 277–352.
32 D. Pum and U. B. Sleytr, *Trends Biotechnol.*, 1999, **17**(1), 8–12.
33 M. Sara and U. B. Sleytr, *Prog. Biophys. Mol. Biol.*, 1996, **65**(1–2), 83–111.
34 M. Sara and U. B. Sleytr, *Micron*, 1996, **27**(2), 141–56.
35 U. B. Sleytr, P. Messner, P. Pum and M. Sára, *Angew. Chem., Int. Ed.*, 1999, **38**, 1034–1054.
36 U. B. Sleytr, M. Sára, D. Pum, B. Schuster, P. Messner and C. Schäffer, Self Assembly Protein Systems: Microbial S-Layers, in *Biopolymers*, A. S. F. Steinbüchel, Ed. Wiley-VCH: Weinheim, Germany, 2002, 7, 285–338.
37 U. B. Sleytr, M. Sára, D. Pum and B. Schuster, *Crystalline bacterial cell surface layers (S layers): a versatile self-assembly system*, CRC Press, Taylor & Francis Group: Boca Raton, FL, 2005, 2, pp. 583–616.
38 A. Breitwieser, S. Küpcü, S. Howorka, S. Weigert, C. Langer, K. Hoffmann-Sommergruber, O. Scheiner, U. B. Sleytr and M. Sára, *Biotechniques*, 1996, **21**(5), 918–258.
39 S. Küpcü, U. B. Sleytr and M. Sára, *J. Immunol. Methods*, 1996, **196**(1), 73–84.
40 C. Völlenkle, S. Weigert, N. Ilk, E. M. Egelseer, V. Weber, F. Loth, D. Falkenhagen, U. B. Sleytr and M. Sára, *Appl. Environ. Microbiol.*, 2004, **70**, 1514–1521.
41 M. Pleschberger, D. Saerens, S. Weigert, U. B. Sleytr, S. Muyldermans, M. Sára and E. M. Egelseer, *Bioconjugate Chem.*, 2004, **15**, 664–671.
42 U. B. Sleytr, E. M. Egelseer, N. Ilk, D. Pum and B. Schuster, *FEBS J.*, 2007, **274**(2), 323–334.
43 N. Ilk, E. M. Egelseer, J. Ferner-Ortner, S. Küpcü, D. Pum, B. Schuster and U. B. Sleytr, *Colloids Surf., A*, 2008, **321**, 163–167.
44 C. Weiner, M. Sára, G. Dasgupta and U. B. Sleytr, *Biotechnol. Bioeng.*, 1994, **44**(1), 55–65.
45 S. Weigert and M. Sára, *J. Membr. Sci.*, 1996, **121**(2), 185–196.
46 S. Küpcü, M. Sára and U. B. Sleytr, *J. Membr. Sci.*, 1991, **61**, 167–175.
47 M. Sára, D. Pum and U. B. Sleytr, *J. Bacteriol.*, 1992, **174**, 3487–3493.
48 S. Küpcü, M. Sára and U. B. Sleytr, *Desalination*, 1993, **90**, 65–76.
49 U. B. Sleytr, M. Sára, Z. Küpcü and P. Messner, *Arch. Microbiol.*, 1986, **146**(1), 19–24.
50 J. Dostálek, A. Kasry and W. Knoll, *Plasmonics*, 2007, **2**(3), 97–106.
51 P. C. C. K. Patel and D. D. Meng, *JALA*, 2010, **15**(2), 114–119.
52 C. Gao, G. Li, H. Xue, W. Yang, F. Zhang and S. Jiang, *Biomaterials*, 2010, **31**(7), 1486–1492.
53 X. Hou and M. Holmberg, *Langmuir*, 2010, **26**(2), 938–942.
54 J. C. Meredith, *J. Mater. Chem.*, 2009, **19**, 34–45.
55 E. S. Györvary, O. Stein, D. Pum and U. B. Sleytr, *J. Microsc.*, 2003, **212**, 300–306.
56 J. L. Toca-Herrera, R. Krastev, V. Bosio, S. Küpcü, D. Pum, A. Fery, M. Sára and U. B. Sleytr, *Small*, 2005, **1**(3), 339–348.
57 M. K. Liu, P. Li and J. C. Giddings, *Protein Sci.*, 1993, **2**(9), 1520–31.